PHYSICAL REVIEW LETTERS **124,** 037801 (2020)

Editors' Suggestion

Ferroelectric-Ferroelastic Phase Transition in a Nematic Liquid Crystal

Nerea Sebastián,[1,*] Luka Cmok,[1] Richard J. Mandle,[2] María Rosario de la Fuente,[3] Irena Drevenšek Olenik,[1,4]
Martin Čopič,[1,4] and Alenka Mertelj[1,†]
[1]*Jožef Stefan Institute, SI-1000 Ljubljana, Slovenia*
[2]*Department of Chemistry, University of York, York YO10 5DD, United Kingdom*
[3]*Department of Applied Physics II, University of the Basque Country (UPV/EHU), Apdo.644-48080 Bilbao, Spain*
[4]*University of Ljubljana, Faculty of Mathematics and Physics, SI-1000, Ljubljana, Slovenia*

(Received 10 October 2019; published 21 January 2020)

Ferroelectric ordering in liquids is a fundamental question of physics. Here, we show that ferroelectric ordering of the molecules causes the formation of recently reported splay nematic liquid-crystalline phase. As shown by dielectric spectroscopy, the transition between the uniaxial and the splay nematic phase has the characteristics of a ferroelectric phase transition, which drives an orientational ferroelastic transition via flexoelectric coupling. The polarity of the splay phase was proven by second harmonic generation imaging, which additionally allowed for determination of the splay modulation period to be of the order of 5–10 microns, also confirmed by polarized optical microscopy. The observations can be quantitatively described by a Landau–de Gennes type of macroscopic theory.

DOI: 10.1103/PhysRevLett.124.037801

A ferroelectric fluid, and more specifically a ferroelectric nematic phase, is of great fundamental and practical interest. Nematic phases retain truly 3D fluidity as their molecules exhibit only orientational but no positional order. Molecular shape is of key importance on determining the occurrence of the different mesophases. While highly symmetrical rodlike molecules give rise to a uniaxial nematic phase, complex molecular shapes may promote nematic phases with higher orientational order as, for example, biaxial [1] or twist-bend nematic phases [2]. On the other hand, chiral molecules, beside the chiral nematic phase, also form three "blue" phases. Although theoretical works anticipate that polar order is more likely to occur in systems made of disklike constituents [3,4], for those consisting of pear- or wedge-shaped molecules, softening of the splay elastic constant was predicted [5] and the occurrence of the splayed polar nematic phase was theoretically demonstrated [6,7]. Although the possibility of a ferroelectric nematic phase was already envisioned by Born [8], experimental evidence has only been observed in some polymer liquid crystals [9], while in low molecular mass materials it has until now eluded experimental discovery.

The so-called splay nematic phase was just recently discovered [10,11] to appear in materials made of molecules with a large dipole moment and a lateral group, which results in a slightly wedge molecular shape [Fig. 1(a)] [12,13]. These materials exhibit two distinct nematic mesophases, the usual uniaxial nematic phase and the lower temperature splay nematic phase. The weakly first order phase transition between the phases is accompanied by a significant pretransitional behavior, manifested as strong splay orientational fluctuations. The transition is driven by instability towards splay orientational deformation, which leads

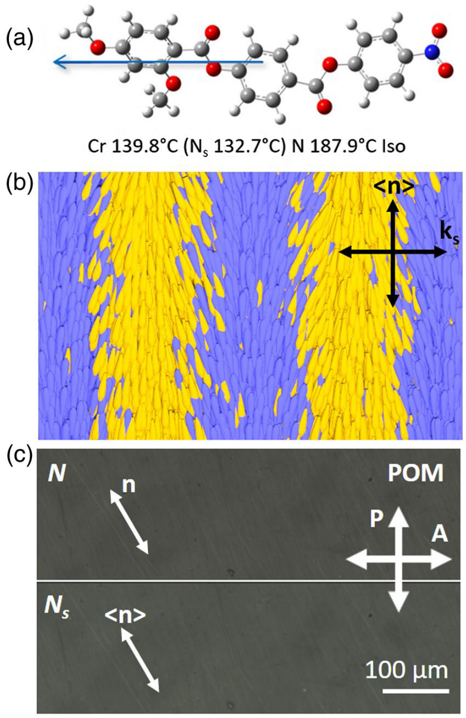

FIG. 1. (a) Schematic of a molecule of RM734 and its phase sequence. (b) Schematic of the splay phase, where different colors denote molecular orientation either along $\mathbf{n}$ or $-\mathbf{n}$. $\mathbf{k}_s$ denotes the splay wave vector. (c) POM images of RM734 in a homogeneous in-plane alignment cell in N and N_s phases (thickness 20 μm) cell.

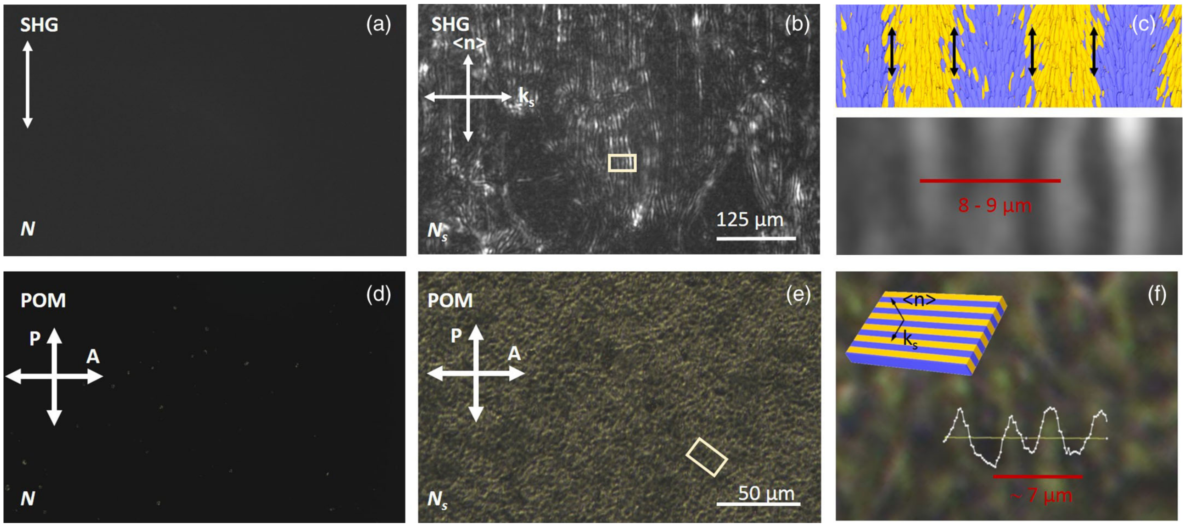

FIG. 2. (a)–(c) SHG microscopy images in the (a) N phase ($T_{NNs} \sim 2$ K) and (b) transition to the N_s phase ($T_{NNs} \sim -0.5$ K) in a planar cell (thickness 20 μm). An enlarged section from (b) is shown in (c) and compared with the proposed structure. (d)–(f) Polarization microscopy images in the (d) N ($T_{NNs} \sim 10$ K) phase and (e) N_s phase ($T_{NNs} \sim -10$ K) for a cell with bare ITO electrodes (thickness 20 μm). An enlarged section from (e) is shown in (f), where the white dots indicate the mean intensity across that section. Rectangles (b) and (e) correspond to the enlarged images in (c) and (f), respectively.

to a periodically splayed structure. Because the splay nematic phase in planar confinement appears optically homogeneous, it was speculated that the modulation period of the splay phase was of nm size similarly as the modulation of the twist bend nematic phase [14,15].

Here, we experimentally demonstrate that the splay modulation is of the order of microns and that the phase transition to the splay nematic phase is a ferroelectric-ferroelastic transition, in which flexoelectric coupling causes simultaneous occurrence of diverging behavior of electric susceptibility and of instability towards splay deformation.

The usual uniaxial nematic phase (N) is nonpolar, and the average orientation of the molecules is described by a unit vector, director $\mathbf{n}$, which has inversion symmetry $\mathbf{n} \equiv -\mathbf{n}$. In the splay nematic phase (N_s), the director exhibits a modulated splayed structure [Fig. 1(b)] that is biaxial and can be described by the average orientation of the director $\langle \mathbf{n} \rangle$, the splay wave vector $\mathbf{k}_s$, and the modulation period $\Lambda = 2\pi/|\mathbf{k}_s|$. Additionally, the splay nematic phase exhibits electric polarization $\mathbf{P}$, whose magnitude oscillates along the splay direction. In liquid crystal (LC) cells with homogeneous in-plane alignment, the well-oriented sample optically looks very similar in both phases [Fig. 1(c)] [10].

As second harmonic generation (SHG) can only be observed in structures with no center of inversion symmetry, in particular in polar structures, it is a very sensitive technique to detect system polarity. Thus, we proved the appearance of polar order during the N-N_s transition by SHG microscopy. In the experiment, a layer of RM734 in a LC cell (Instec Inc., thickness 20 μm), is illuminated by pulsed laser light ($\lambda = 800$ nm, pulse length: 100 fs, repetition rate: 1 kHz) and imaged with a system composed of a 20× microscopy objective and a CMOS camera (see detailed description in the Supplemental Material [16]).

In the N phase, the SHG image appears completely dark, as expected for a homogeneously oriented nonpolar nematic liquid crystal [Fig. 2(a)]. On cooling, the transition to the splay phase is characterized by a sudden strong SHG signal [coinciding with the destabilization of homogeneous orientation observed by polarization microscopy (POM) [10]]. During the transition, the SHG image clearly shows a periodic stripped texture [Fig. 2(b)] with a periodicity of around 8 to 9 μm perpendicular to the rubbing direction. In agreement with the proposed phase structure, the bright regions correspond to the splayed deformation and the dark lines to those where $\mathbf{P} = 0$ [Fig. 2(c)]. The SHG activity clearly demonstrates that the N_s phase is polar. Right below the $N - N_s$ transition, the splay wave vector orients perpendicularly to the plane of the sample and the periodic structure is only observed around defects [Supplemental Material [16], Fig. S1(c)].

Interestingly, while in the cells treated for perpendicular alignment of $\mathbf{n}$, random in-plane alignment was obtained [10], in nontreated ITO cells, $\mathbf{n}$ in the N phase aligns out of plane [Fig. 2(d)]. In the N_s phase, the $\mathbf{k}_s$ lays then in the plane of the sample, but there is no preferred in-plane orientation for it, so its direction changes with position, resulting in a disordered structure discernable after the phase stabilization. In a POM image, small regions having a regular modulation with a periodicity of about 7 μm are observed [Figs. 2(e)–2(f)], in correspondence with SHG observations in the transition and around defect lines.

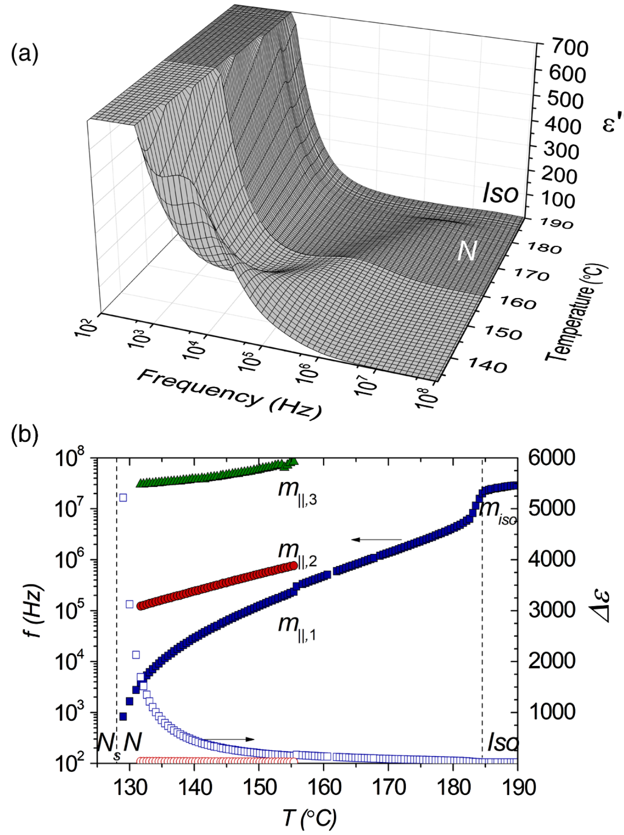

FIG. 3. (a) 3D plot of the dielectric losses ε'' vs temperature and frequency. (b) Temperature dependence of the relaxation frequencies and strengths of the different processes in the isotropic and nematic phases.

To gain insight into the polarization mechanisms involved in the N-N_s phase transition, we measured the complex permittivity $\varepsilon(\omega) = \varepsilon'(\omega) - i\varepsilon''(\omega)$ in the frequency range 10 Hz–110 MHz (see Supplemental Material [16] for a detailed description). The sample consisted of two circular gold-plated brass electrodes of 5 mm diameter and separated by 50 μm thick silica spacers. The untreated gold surfaces spontaneously gave rise to perpendicular alignment, and thus, a parallel component of the permittivity was measured [Fig. 3(a)]. The measuring oscillator level was set to 10 $\mathrm{mV_{rms}}$ and measurements were performed on cooling. The probe electric field was low enough for the measurements to be in the linear regime in the N phase. However, in the N_s phase, optical switching was detected for fields as low as the employed probe field, and thus, interpretation of results is challenging and will be reported elsewhere.

Characteristic frequency and amplitude of each process are obtained by fitting $\varepsilon(\omega)$ to the Havriliak-Negami (HN) equation [17,18] (see Supplemental Material [16] for fit examples) (Fig. 3). In the isotropic phase (I), a single relaxation process (m_{iso}) is detected with frequency of the order of 20 MHz for the rigid dipolar molecule rotating in the isotropic environment. $\Delta\varepsilon_{\mathrm{iso}} \sim 17$ is in agreement with the large calculated molecular longitudinal dipole moment ~11.4 D [10,19]. In the N phase, immediately after the I-N transition and in the frequency range studied, a single process $m_{\|,1}$ is detected with lower frequency and larger amplitude than in the I phase. On cooling $\Delta\varepsilon_{\|,1}$ steadily increases and a broadening of the relaxation can be detected. Far below T_{IN} it is possible to resolve such broadening into a second process $m_{\|,2}$ with lower strength ($\Delta\varepsilon_{\|,2} \sim 40$), which becomes clear by analyzing $d\varepsilon'(f)/d[\log(f)]$ vs $\log(f)$(SI). It appears that close to T_{IN} the detected mode, in line with usual nematic behavior for molecules with longitudinal dipole moment, can be attributed to molecular rotations around the short molecular axis. However, collective behavior starts to develop on lowering the temperature, as evidenced by the strength increase. As collective motions slow down faster than the molecular process, at around 160 °C, both processes become distinguishable, being then possible to attribute $m_{\|,2}$ to the molecular rotations around the short molecular axis and $m_{\|,1}$ to a collective movement of dipole moments. Additionally, a third mode $m_{\|,3}$ is detected in the higher part of the frequency range (~1–10 MHz). The strength of this mode is very small compared to the main contributions, and thus both its frequency and its amplitude as depicted in Fig. 3(b) and Fig. SI6 in Supplemental Material [16], are just tentative. This mode, by frequency and amplitude, can be attributed to the rotation around the molecular long axis, as described by the Nordio-Rigatti-Segre theory [20]. On further approaching the N-N_s phase transition, softening of the $m_{\|,1}$ mode is evidenced by the strong decrease of the relaxation frequency and divergence of $\Delta\varepsilon_{\|,1}$, as the result of molecular motions becoming collective. Complete condensation of the mode could not be observed as, close to the transition, $m_{\|,1}$ is masked by conductivity effects and can only be followed until 2 degrees before the transition, for which $f \sim 800$ Hz.

Theoretically, this transition between the N and N_s phases can be described by a Landau–de Gennes type of the free energy [10,21]. The order parameter of the nematic phase is a tensor and to understand the temperature behavior of the elastic constants on a larger temperature interval a tensor description is necessary [21]. However, in the case of the N-N_s transition, the critical behavior is limited to the temperature range where the scalar order parameter is approximately constant [11], and the description of the nematic phase by $\mathbf{n}$ is sufficient. In the N_s phase, as demonstrated experimentally by SHG, the inversion symmetry is broken, which means that an additional vector order parameter is needed. If molecules have dipole moments with a component along the symmetry axis, as is in our case, then the vector order parameter is the electric polarization $\mathbf{P}$. However, in general, the origin of the order parameter vector is not necessarily the electric polarization, but can be, for example, the shape of the molecule [5,22]. In the N phase, splay or bend orientational deformations give rise to flexoelectric polarization, which is the result of the coupling between $\mathbf{P}$ and the deformation of $\mathbf{n}$ [23]. It has been shown that this coupling can be a driving mechanism for a transition from the uniaxial to a modulated nematic phase [10,22,24]. The free energy density with minimum number of terms necessary for the description of the N-N_s transition is then

$$f = \frac{1}{2}K_1(\nabla\cdot\mathbf{n})^2 + \frac{1}{2}K_3(\mathbf{n}\times(\nabla\times\mathbf{n}))^2 - \gamma\mathbf{n}(\nabla\cdot\mathbf{n})\cdot\mathbf{P} + \frac{1}{2}t\mathbf{P}\cdot\mathbf{P} + \frac{1}{2}b(\nabla\mathbf{P})^2. \tag{1}$$

Here, the first two terms are the usual Frank elastic free energy terms, where K_1 and K_3 are the splay and the bend orientational elastic constants, respectively. The third term describes the coupling between the splay deformation and the electric polarization, where γ is a bare splay flexoelectric coefficient. The last two terms are the lowest by symmetry allowed terms in $\mathbf{P}$ and $\partial P_i/\partial x_j$. In our case, the molecular dipole moment is along the molecular long axis, so $\mathbf{P} = P\mathbf{n}$. Although the N-N_s phase transition described by Eq. (1) is a second order phase transition, it can be extended to describe a weakly first order phase transition by adding higher order terms [25].

Because of the flexoelectric coupling, the orientational fluctuations of $\mathbf{n}$ are coupled with the fluctuations of $\mathbf{P}$, which causes the existence of two branches of the splay eigenmodes (see Supplemental Material [16] for details): a hydrodynamic mode, which is mostly a director mode, and an optic mode, which is predominantly a polarization mode. By dielectric spectroscopy, the polarization eigenmode at $q = 0$ is measured. Its relaxation rate is $t/(2\eta_P)$, where η_P is the dissipation coefficient for $\mathbf{P}$, and the square amplitude of fluctuations is $\langle P^2\rangle = 2k_BT/(Vt)$, where V is the volume of the sample. $\langle P^2\rangle$ is proportional to $\Delta\varepsilon_{\parallel,1}$ (see Supplemental Material [16]) [26].

The flexoelectric coupling in general causes that the splay elastic constant measured in the experiments is rescaled as $K_{1,\mathrm{eff}} = K_1 - \gamma^2/t$ (see Supplemental Material [16] and Refs. [10,21]). If polar order is not favorable, then t is large and the flexoelectric coupling barely affects the measured value of K_1. However, when approaching the ferroelectric phase transition, t decreases with temperature and, in a usual Landau description, the transition to a ferroelectric phase would happen when t becomes negative [25]. However, if the flexoelectric coupling exists, then the phase will become unstable towards splay deformation at a positive, critical value $t_c = \gamma^2/K_1$, i.e., before t becomes negative. In general, the coefficient t is related to the electric susceptibility χ, as $t = 1/(\varepsilon_0\chi)$, where ε_0 is the vacuum permittivity. In our case, the collective polarization $m_{\parallel,1}$ mode is the one that drives the ferroelectric transition and its contribution to the susceptibility determines $t = (\varepsilon_0\Delta\varepsilon_{\parallel,1})^{-1}$ (see Supplemental Material [16]), so the effective splay elastic constant can be written

$$K_{1,\mathrm{eff}} = K_1 - \varepsilon_0\gamma^2\Delta\varepsilon_{\parallel,1} \tag{2}$$

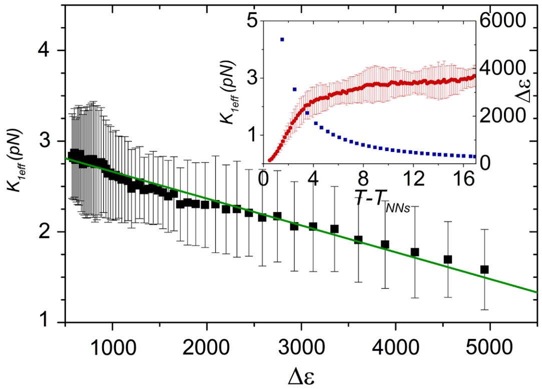

FIG. 4. Measured values of $K_{1,\mathrm{eff}}$ vs interpolated values of $\Delta\varepsilon_{\parallel,1}$. Inset shows the temperature dependence of both K_1 and $\Delta\varepsilon_{\parallel,1}$ a few degrees above the transition to the N_s phase. The green line corresponds to the linear fit from which $\gamma = 0.006$ V is obtained.

The dependence of the measured effective splay elastic constant [10] on $\Delta\varepsilon_{\parallel,1}$ (Fig. 4) substantiates the linear dependency predicted by Eq. (2). The linear fits yields the values of $\gamma = 0.006$ V, $K_1 = 3$ pN, and, $\varepsilon_0 t_c = 10^{-4}$.

The modulation period just below the N-N_s phase transition is determined by the ratio of the elastic constants K_1 and b, and the flexoelectric coefficient: $\Lambda = 2\pi\sqrt{3bK_1/(\gamma^2\Delta t_n)}$, where $\Delta t_n = 1 - t/t_c$ [10]. If flexoelectric coupling is large, then the modulation period is small and vice versa. In our case, the value of the bare flexoelectric coefficient γ is very small and so the modulation period is in the μm range. In this size range, it should be visible in POM imaging; however, there are several effects that hinder such observation. The SHG imaging has shown that in LC cells treated for homogeneous in-plane alignment, after the stabilization of the phase, the splay wave vector tends to align perpendicularly to the plane of the cell, and a periodic structure is only seen around defects. In polarizing microscopy, such periodic structure around defects cannot be distinguished (Supplemental Material [16], Fig. S1. c). A possible reason is that the splay deformation is so small that the scattering from orientational fluctuations, which are in such geometry strongly expressed, masks it. Additionally, the deformation of $\mathbf{n}$ close to the defect causes diffraction of light, which again hinders POM imaging. In cells without an alignment layer, in which for the N phase, $\mathbf{n}$ aligns perpendicularly to the sample plane, in the N_s phase, the modulation is visible [Figs. 2(e)–2(f)] as this case corresponds to the geometry in which fluctuations do not cause scattering of light [27]. Observed periodicity and sample confinement are of the same order and, consequently, determination of the temperature dependence of the periodicity requires additional methods. However, our observations suggest that it remains of the same order down to few degrees below the transition. In agreement with these observations, the splay modulation period in the order of μm was also very recently observed optically in a two-component mixture [28]. It should also be mentioned that a phase showing similar textures and polarity was recently observed in a liquid crystal compound with a 1,3-dioxane unit [29].

Here it is important to note that the ferroelectric phase transition described by Eq. (1) will always be accompanied by a ferroelastic transition even if the flexoelectric coupling is very small. This case is very similar to ferroelectric-ferroelastic phase transitions in some solid materials, in which linear coupling between strain and polarization is by symmetry allowed, as, for example, in KDP [30]. The main difference between the transition in a solid or in a nematic liquid crystal is in the deformation type, which is a strain in the former case, while in the latter, it is orientational. While strain can be homogeneous, it is not possible to fill the space with homogeneous splay, and, consequently, a modulated structure is formed. The appearance of simultaneous polar order and splay deformation as a consequence of flexoelectric coupling was already theoretically predicted by Pleiner *et al.* [31,32].

In conclusion, we have experimentally shown that in the recently discovered splay nematic phase, the modulation period is of macroscopic size. The transition from the uniaxial to the splay nematic phase is a ferroelectric phase transition, which is evidenced by the divergent behavior of electric susceptibility, and is, due to the flexoelectric coupling, accompanied by orientational ferroelastic transition. The observed behavior raises fundamental questions about polar order in liquids, as, for example, what combination of molecular charge distribution and shape is necessary that the molecules will on average orient in the same direction while still remaining in a liquid state. And, would any such combinations allow for realization of a homogeneous uniaxial ferroelectric nematic phase or is it essential that ferroelectric ordering in a nematic liquid crystal is accompanied by orientational deformation.

N. S., I. D. O., M. Č., and A. M. acknowledge the financial support from the Slovenian Research Agency (research core Funding No. P1-0192). L. C. acknowledges support from Slovenian Ministry of Education, Science and Sport (MIZŠ) & ERDF (project OPTIGRAD). R. J. M. acknowledges the EPSRC (UK) and QinetiQ for the award of an ICASE studentship. M. R. F. acknowledges support from University of the Basque Country UPV/EHU: GIU18/146.

---

[*] Corresponding author.
nerea.sebastian@ijs.si

[†] Corresponding author.
alenka.mertelj@ijs.si

[1] Biaxial Nematic Liquid Crystals: Theory, Simulation, and Experiment Soft Matter, in *General & Introductory Materials Science*, edited by G. R. Luckhurst and T. J. Sluckin (Wiley, West Sussex, 2015).

[2] K. Adlem, M. Čopič, G. R. Luckhurst, A. Mertelj, O. Parri, R. M. Richardson, B. D. Snow, B. A. Timimi, R. P. Tuffin, and D. Wilkes, Chemically induced twist-bend nematic liquid crystals, liquid crystal dimers, and negative elastic constants, Phys. Rev. E **88**, 022503 (2013).

[3] P. Palffy-Muhoray, M. A. Lee, and R. G. Petschek, Ferroelectric Nematic Liquid Crystals: Realizability and Molecular Constraints, Phys. Rev. Lett. **60**, 2303 (1988).

[4] F. Bisi, A. M. Sonnet, and E. G. Virga, Steric effects in a mean-field model for polar nematic liquid crystals, Phys. Rev. E **82**, 041709 (2010).

[5] P. D. Gregorio, E. Frezza, C. Greco, and A. Ferrarini, Density functional theory of nematic elasticity: Softening from the polar order, Soft Matter **12**, 5188 (2016).

[6] S. Dhakal and J. V. Selinger, Statistical mechanics of splay flexoelectricity in nematic liquid crystals, Phys. Rev. E **81**, 031704 (2010).

[7] R. Berardi, M. Ricci, and C. Zannoni, Ferroelectric and structured phases from polar tapered mesogens, Ferroelectrics **309**, 3 (2004).

[8] M. Born, Über anisotrope Flüssigkeiten. Versuch einer Theorie der flüssigen Kristalle und des elektrischen KERR-Effekts in Flüssigkeiten, Sitzungsber. Preuss. Akad Wiss. **30**, 614 (1916).

[9] H. Takezoe, Polar liquid crystals—ferro, antiferro, banana, and columnar—, Mol. Cryst. Liq. Cryst. **646**, 46 (2017).

[10] A. Mertelj, L. Cmok, N. Sebastián, R. J. Mandle, R. R. Parker, A. C. Whitwood, J. W. Goodby, and M. Čopič, Splay Nematic Phase, Phys. Rev. X **8**, 041025 (2018).

[11] R. J. Mandle and A. Mertelj, Orientational order in the splay nematic ground state, Phys. Chem. Chem. Phys. **21**, 18769 (2019).

[12] R. J. Mandle, S. J. Cowling, and J. W. Goodby, A nematic to nematic transformation exhibited by a rod-like liquid crystal, Phys. Chem. Chem. Phys. **19**, 11429 (2017).

[13] R. J. Mandle, S. J. Cowling, and J. W. Goodby, Rational design of rod-like liquid crystals exhibiting two nematic phases, Chem. Eur. J. **23**, 14554 (2017).

[14] V. Borshch, Y.-K. Kim, J. Xiang, M. Gao, A. Jákli, V. P. Panov, J. K. Vij, C. T. Imrie, M. G. Tamba, G. H. Mehl, and O. D. Lavrentovich, Nematic twist-bend phase with nanoscale modulation of molecular orientation, Nat. Commun. **4**, 2635 (2013).

[15] D. Chen, J. H. Porada, J. B. Hooper, A. Klittnick, Y. Shen, M. R. Tuchband, E. Korblova, D. Bedrov, D. M. Walba, M. A. Glaser, J. E. Maclennan, and N. A. Clark, Chiral heliconical ground state of nanoscale pitch in a nematic liquid crystal of achiral molecular dimers, Proc. Natl. Acad. Sci. U.S.A. **110**, 15931 (2013).

[16] See Supplemental Material at http://link.aps.org/supplemental/10.1103/PhysRevLett.124.037801 for a comparison of SHG and POM images around a defect line/wall.

[17] S. Havriliak and S. Negami, A complex plane analysis of α-dispersions in some polymer systems, J. Polym. Sci. Part C **14**, 99 (1966).

[18] F. Kremer and A. Schönhals, Analysis of dielectric spectra, in *Broadband Dielectric Spectroscopy*, edited by (Springer-Verlag, Berlin Heidelberg, 2003), pp. 59–98.

[19] M. J. Frisch *et al. Gaussian 09, Revision A.02* (Gaussian, Inc., Wallingford CT, 2016).

[20] P. L. Nordio, G. Rigatti, and U. Segre, Dielectric relaxation theory in nematic liquids, Mol. Phys. **25**, 129 (1973).

[21] M. Čopič and A. Mertelj, Q-tensor model of twist-bend and splay nematic phases, arXiv:1910.01424.

[22] L. Longa and G. Pająk, Modulated nematic structures induced by chirality and steric polarization, Phys. Rev. E **93**, 040701(R) (2016).

[23] R. B. Meyer, Piezoelectric Effects in Liquid Crystals, Phys. Rev. Lett. **22**, 918 (1969).

[24] S. M. Shamid, S. Dhakal, and J. V. Selinger, Statistical mechanics of bend flexoelectricity and the twist-bend phase in bent-core liquid crystals, Phys. Rev. E **87**, 052503 (2013).

[25] A. F. Devonshire, Theory of ferroelectrics, Adv. Phys. **3**, 85 (1954).

[26] M. R. de la Fuente and D. Dunmur, *Dielectric Properties of Liquid Crystals, in Handbook of Liquid Crystals*, (Wiley-VCH Verlag GmbH & Co. KGaA, Weinheim, 2014), pp. 1–46.

[27] P. G. de Gennes and J. Prost, *The Physics of Liquid Crystals* 2nd ed. (Clarendon Press, Oxford, 1995).

[28] P. L. M. Connor and R. J. Mandle, Chemically induced splay nematic phase with micron scale periodicity, Soft Matter **16**, 324 (2020).

[29] H. Nishikawa, K. Shiroshita, H. Higuchi, Y. Okumura, Y. Haseba, S. Yamamoto, K. Sago, and H. Kikuchi, A fluid liquid-crystal material with highly polar order, Adv. Mater. **29**, 1702354 (2017).

[30] B. A. Strukov and A. P. Levanyuk, *Ferroelectric Phenomena in Crystals: Physical Foundations* (Springer-Verlag, Berlin Heidelberg, 1998).

[31] H. Pleiner and H. R. Brand, Spontaneous splay phases in polar nematic liquid crystals, Europhys. Lett. **9**, 243 (1989).

[32] H. R. Brand, H. Pleiner, and F. Ziebert, Macroscopic dynamics of polar nematic liquid crystals, Phys. Rev. E **74**, 021713 (2006).